Wirelessly-Powered Wireless Sensor Platform

T. Paing, J. Morroni, A. Dolgov, J. Shin, J. Brannan, R. Zane, Z. Popovic

University of Colorado at Boulder, CO, 80308, USA

{thurein.paing, jeffrey.morroni, arseny.dolgov, shinj, joseph.hagerty, zane, zoya}@colorado.edu

***Abstract*— This paper presents a low-power (~10μW) 2.45-GHz wireless sensor platform consisting of a three-axis accelerometer, thermometer and skin conductivity sensor. The sensor is powered wirelessly from a distance of around 3-4m with narrowband 2.45-GHz dual-polarized low power density radiation of around 100μW/cm^2. Efficient power management enables the powering function to be independent of the wireless transmission and sensor data gathering. The sensor platform does not require battery replacements, and is intended for low-maintenance assistive technology, elder-care and medical applications.**

I. Introduction

In the past few decades, a considerable amount of work has been done in the area of wireless powering, including RF inductive powering for short ranges [1], high power density directive powering in the microwave frequency range [2-4], as well as low-power near-field interrogation with RFID tags, and medium- and low-power density powering of low-power sensors [5-8]. This paper addresses low-power sensor applications as described in Fig.1. One or more sensors collect data, which is modulated onto a microwave carrier and transmitted by a low-power transmitter with some duty cycle. Independently, continuously or in bursts, RF power is received and rectified, providing DC power to the sensor and associated electronics. The data transmission and powering can be, but are not necessarily at the same frequency. Further, the powering can be accomplished simultaneously at different frequencies [8]. A microcontroller manages the received power to optimally charge an on-board storage device. The sensor and wireless transmission is also controlled through this device. The goal of this paper is to demonstrate that integrated design of the powering and sensor functions is required for minimizing overall power consumption.

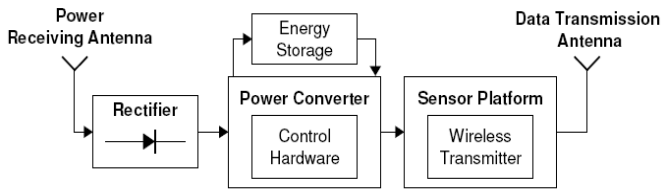

Fig. 1 Block diagram of wirelessly-powered low-power wireless sensor. Sensors collect data which is then transmitted from a low-power wireless transmitter. Power is received through RF waves incident on a powering antenna integrated with a rectifier (rectenna). A digitally-controlled power-management circuit optimally charges an energy storage device which provides power to the sensor platform.

In the remainder of the paper, the separate block diagrams from Fig.1 are first detailed, followed by results for the entire integrated wireless sensor. This sensor does not require battery replacement. Several applications for this type of low-power low-maintenance sensors exist in the fields of assistive technology and elderly care.

II. Wireless Power Reception – the Rectenna

The rectenna design is determined by space constraints and the electromagnetic environment. In the work presented here, one or more medium-power semi-directional transmitters illuminate a range in space, with multipath present. The incident power density is known approximately, but there are multipath effects that change the polarization and spatial distribution of power density. The transmitters described here work operate at a single ISM-band frequency (2.45GHz).

When characterizing the rectenna, it is illuminated from a known distance and incidence angle with a known frequency, polarization and power; thus the incident power density $S(\theta,\phi,f,t)$ is known. The geometrical electrical area of the antenna is known at the frequency used for powering. This is generally larger than the effective area and therefore overestimates the received RF power. The DC power is then measured as a function of the DC load impedance (resistance) and the estimated conversion efficiency is found as P_{RF}/P_{DC}. Since the DC power is measured directly, and the RF power is over-estimated, the resulting efficiency will be an under-estimate.

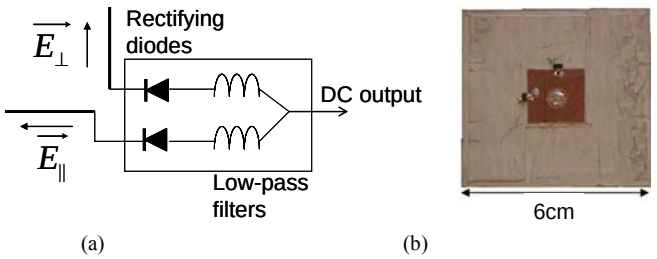

Fig. 2 (a) Block diagram of a dual-polarized rectenna and (b) photograph of a 2.4GHz dual-polarized patch rectenna. Two rectifying diodes are connected to the orthogonally polarized radiating edges of the patch, and the DC power is extracted through the via positioned at the RF voltage null of the antenna.

The block diagram of a single rectenna element is shown in Fig.2a and consists of a dual-polarized antenna, with each port corresponding to one of two orthogonal polarizations connected to a rectifying Schottky diode. The diodes rectify the RF power in the two orthogonal polarizations

independently, and the DC power is added upon rectification and filtering. Due to the statistical nature of multipath propagation, the DC power obtained in this manner does not vary as dramatically as would be the case for a single-polarized rectenna. Fig.2b shows the photograph of a dual-linearly polarized patch antenna at 2.4GHz fabricated on a high-permittivity substrate ($\varepsilon_r \approx 10$) for reduced size, and with two Schottky diodes (Avago HSMS-8101) connected to each radiating edge. The DC is extracted through a via in the RF voltage null of the patch, which provides some RF filtering, and is followed by a two-pole LC low-pass filter.

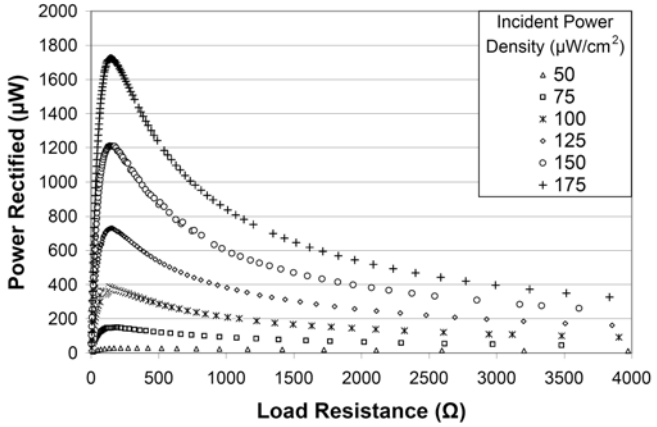

Fig. 3 Measured output DC power from a rectenna as a function of DC load resistance over a range of low-level incident power densities. The incident plane wave is linearly polarized along one of the two patch edges.

A measurement was also performed to confirm the fact that the DC power is produced with less variation when a dual polarized rectenna is used. The results are shown in Fig.4, where for a linearly polarized incident wave with constant power density of $170\mu\text{W/cm}^2$, the rectenna orientation is varied as indicated below the histogram. It is shown that compared to a linearly polarized patch rectenna, the DC power is larger but more importantly, the variation of received power is reduced by approximately a factor of two. This rectenna operates with incident power levels as low as $10\mu\text{W/cm}^2$ and we show in this paper that it is capable of powering a low-power wireless sensor and all associated electronics.

The power provided by the rectenna is stored in either a low-leakage current capacitor or thin-film battery. In either case, the DC power should not vary for optimal charging, requiring a power management circuit. In addition, the power management circuit should present an optimal load to the rectenna for best overall efficiency. Thus the rectenna is characterized by varying the DC load for different incident power densities, and the result for a linearly-polarized incident wave on broadside is shown in Fig.3. There is an optimal load resistance on the order of a few hundred ohms, which varies with incident power density due to the nonlinear I-V curve of the diodes.

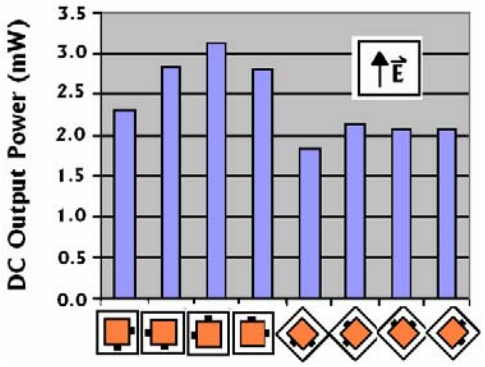

Fig. 4 Measured histogram of DC power levels for an incident power level of $170\mu\text{m/cm}^2$ for different orientations of the dual-polarized rectenna element, corresponding to different incident polarizations. The incident RF power is linearly polarized.

III. Power Management and Storage

In order to optimally load the rectenna over a range of low incident power levels, a power converter is designed to emulate a constant positive impedance based on the rectenna curves from Fig.3. This converter schematic is shown in Fig.5a. The peak power point occurs at a single load point over the full range of incident power levels.

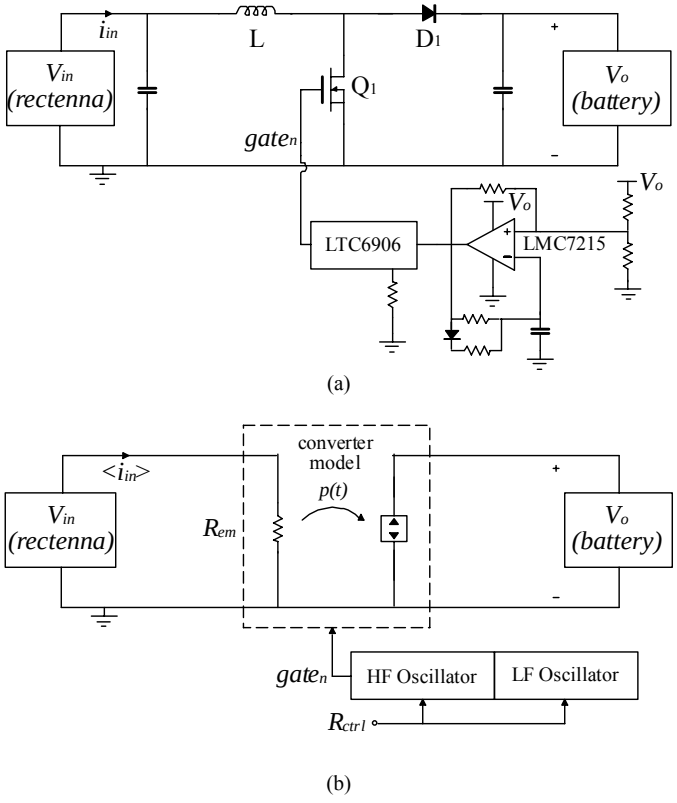

Fig. 5. (a) Boost converter schematic with simplified control circuitry to achieve near constant resistor emulation. (b) Block diagram of converter model and associated control.

The power converter in Fig.5a is a boost converter topology operating in pulsed fixed-frequency discontinuous conduction mode (DCM). Using a converter model (Fig.5b), the emulated resistance is shown in [10] to be

$$R_{em} = R_{ctrl}\left(\frac{M-1}{M}\right),$$

where $M = \frac{V_o}{V_{in}}$. Control parameters are fed into the two oscillators to generate a gate drive signal, $gate_n$, that drives the transistor Q_1. This signal switches the power converter to emulate a resistance R_{ctrl} with a correction factor. The correction factor, $(M\text{-}1)/M$, can be approximated as unity if $V_{in} << V_o$, which will be the case at the expected incident RF power levels.

Following the design steps in [9] that take into account converter power loss equations, the control parameters fed into the two oscillators are selected to attain R_{ctrl} whilst maximizing converter efficiency. The converter is then built using commercially available discrete components where the control circuitry is powered off the output voltage, V_o.

The converter is tested with the rectenna at its input over a range of incident power levels. A converter efficiency of 61.4% at 70μW output power is achieved while maintaining a near-constant emulated resistance within 10% of the optimal value.

A 4-V thin-film Lithium battery is selected over an ultra-capacitor as the energy storage element, due to its form-factor, greatly improved leakage current, and storage capacity.

IV. Wireless Sensors and Control Electronics

The sensor module consists of a Texas Instruments MSP430 microcontroller unit (MCU) which acquires data from several onboard sensors, including temperature, 3-axis acceleration/inclination and galvanic skin response (GSR) and transmits the information at 2.4 GHz to a receiver station up to 10 meters away in an indoor environment. A breakdown of the corresponding power consumption during the sample-and-transmit cycle is given in Fig 6. The MCU, radio and sensors are optimized for low-power operation, and include fast serial peripheral interface (SPI) and short power-up and settling times to minimize time spent in 'Active' modes.

The sensor module also utilizes an RC network to produce a negative-going edge and provide an interrupt timer to wake up the CPU and begin sampling. Using this timer, the MCU can power down to a current of only 0.1 μA, which significantly reduces the total standby power of the system.

Finally, the sensor module utilizes a rather large 47 μF capacitor at the output of the linear regulator. This capacitor provides sleep power to the MCU between sampling cycles. After the MCU samples the sensors and transmits the data, the regulator is shut down to conserve power. Enough energy remains on the capacitor, though, to power the MCU until it wakes up again. Due to the robust operating range of this specific MCU (1.8 V to 3.6 V), it remains operational and can detect interrupts even when the capacitor voltage drops significantly.

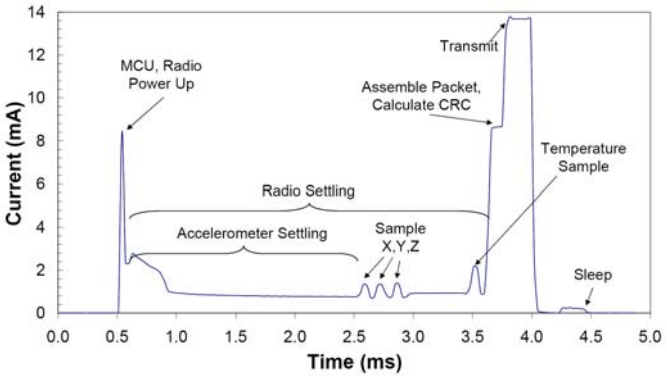

Fig. 6. Sensor module power consumption during one sample-and-transmit cycle. The graph shows the wake-up and settling period of the microcontroller (MCU) and various onboard sensors. The MCU samples and wirelessly transmits sensor data within 4 ms, after which it returns to a low-power 'Sleep' state.

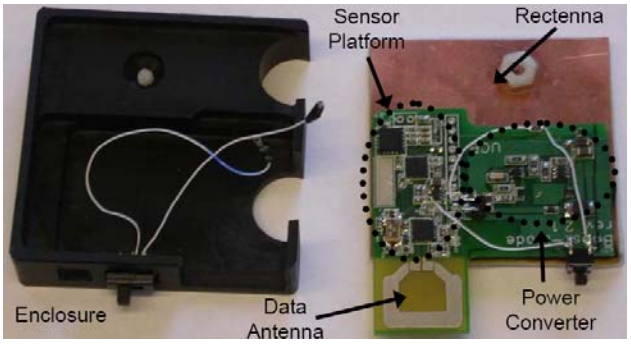

Fig. 7 Photograph of wirelessly powered wireless sensor. The power converter, sensors, controller and transceiver are integrated onto a single PCB and mounted directly above the rectenna with connections underneath the PCB. The separate data-transmitting antenna is a short folded dipole. The size of the package is 6cm x 6cm x 0.8cm.

V. Integrated Wirelessly-Powered Sensor

Fig.7 shows the integrated wirelessly powered sensor with a packaged rectenna, power converter, sensor load and associated electronics. The sensor data link is tested by measuring the number of packets lost divided by packets sent, for varying range. The receiver is connected to a computer, through USB, and relays the data to a LabVIEW interface. The percentage of lost packets, for this specific platform, is less than 5% for distances up to 10m and is independent of transmitter and receiver relative orientations. For larger distances, however, the link is reliable only for co-polarized antennas.

The wireless powering source is accomplished through a transmitter consisting of a Mini-circuits 2.4-GHz VCO (JTOS-3000P) amplified by a Fidelity Comtech 1-W PA (FCI-CCA) feeding a half wavelength monopole antenna. At 1W

output, the wireless sensor is fully powered at a range of 3-4m away from the transmitter.

With the entire system integrated, a comparison between the amount of energy harvested and the amount of energy consumed is required to determine if the system is capable of keeping the battery charged for the given load. Fig. 8 shows the power delivered (left y-axis) by the converter to the battery for a given incident RF power level. Also plotted (right y-axis) is the corresponding maximum sample rate such that the sensor does not consume more power than is delivered. It can be seen that even for extremely low power densities (18 μW/cm^2) incident on the rectenna, the system provides enough power (75 μW) for the wireless sensor to sample at 3 samples/s.

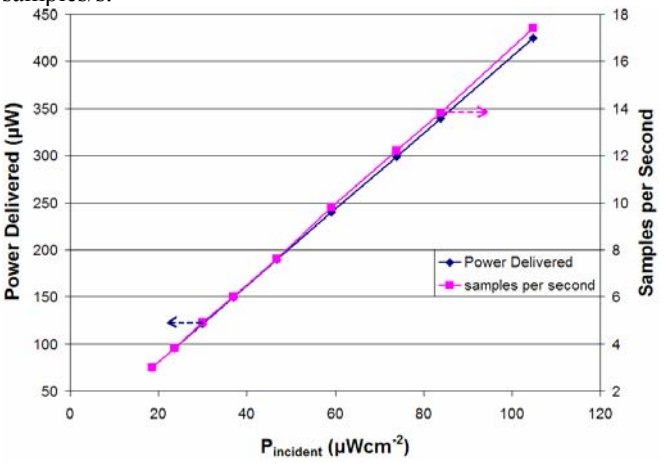

Fig. 8 Power delivered from the converter and the corresponding maximum samples per second for given incident RF power level such that there is no net power consumption.

The LabVIEW user interface, shown in Fig. 9, reports all of the sensor platform readings as well as harvested power, rectenna open circuit voltage, and current battery voltage. This interface is updated at the same rate as the sensor update rate previously described. In summary, we have demonstrated a low-power wireless sensor that does not require battery replacement. The sensor electronics is powered through incident low-power density radiation in an ISM band, enabled by integrated design of the RF and power management circuit.

ACKNOWLEDGMENTS

The authors acknowledge the support of ITN Energy Systems and Luna Innovations for funding under Air Force STTR and Navy SBIR grants, as well as the Coleman Foundation and the Technology Transfer Office at the University of Colorado. Zoya Popovic is also grateful to the German Alexander von Humboldt Stiftung for a Humboldt Research Award which enabled her to spend time at the Technical University in Munich away from regular duties, resulting in much of the initial RF work presented in this paper.

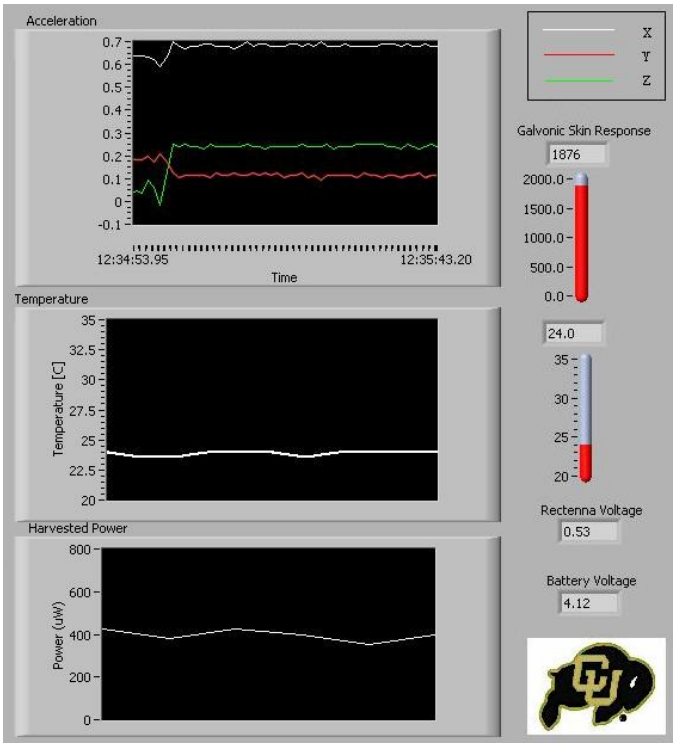

Fig. 9 User interface designed in LabVIEW that reports all data being collected and transmitted by the wirelessly-powered wireless sensor platform.

REFERENCES

[1] W.C. Brown, "The history of power transmission by radio waves," *IEEE Trans. Microwave Theory Techn.* vol.32, no.9, pp. 1230–1242, Sept. 1984.

[2] N. Shinohara and H. Matsumoto, "Experimental study of large rectenna array for microwave energy transmission," *IEEE Trans. Microwave Theory Techn.* vol.46, no. 3, pp. 261–267, Mar. 1998.

[3] J.O. McSpadden, F.E. Little, M.B Duke, and A. Ignatiev, "An in-space wireless energy transmission experiment," *IECEC Energy Conversion Engineering Conf.Proc.*, vol. 1, pp. 468–473, Aug. 1996.

[4] B. Strassner, K. Chang, "A circularly polarized rectifying antenna array for wireless microwave power transmission with over 78% efficiency," *IEEE MTT-S IMS Digest*, pp.1535–1538, 2002.

[5] C. Walsh, S. Rondineau, M. Jankovic, G. Zhao, Z. Popovic, "A Conformal 10-GHz Rectenna for Wireless Powering of Piezoelectric Sensor Electronics," *IEEE 2005 IMS Digest,* Long Beach, June '05.

[6] W.C. Brown, "An experimental low power density rectenna," *IEEE MTT-S IMS Digest*, pp. 197–200, 1991.

[7] J.A Hagerty, Z. Popovic, "An experimental and theoretical characterization of a broadband arbitrarily-polarized rectenna array," *IEEE MTT-S IMS Digest*, vol. 3, pp. 1855– 1858, 2001.

[8] J.A. Hagerty, F. Helmbrecht, W. McCalpin, R. Zane, Z. Popovic, "Recycling ambient microwave energy with broadband antenna arrays," *IEEE Trans. Microwave Theory and Techn.,* pp. 1014-1024, March 2004.

[9] T. S. Paing, R. A. Zane, "Resistor emulation approach to low-power energy harvesting," *Proc. IEEE 37th Power Electron. Spec. Conf.*, Jun. 18-22, 2006, Jeju, S. Korea, pp. 1-7.

[10] A. Dolgov and R. Zane, "Low-Power Wireless Medical Sensor Platform", *Proceedings of the 28th IEEE EMBS Annual International Conference*, New York, NY, 2006, pp. 2067- 2070.